

A Cell-Free Silk Fibroin Biomaterial Strategy Promotes In Situ Cartilage Regeneration Via Programmed Releases of Bioactive Molecules

Zhinan Mao, Xuwei Bi, Chengai Wu, Yufeng Zheng, Xiong Shu,* Sujun Wu,* Juan Guan,* and Robert O. Ritchie

In situ tissue regeneration using cell-free biofunctional scaffolds has been extensively studied as a promising alternative strategy to promote cartilage repair. In this study, a cartilage-biomimetic silk fibroin (SF)-based scaffold with controlled sequential release of two bioactive molecules is developed. Transforming growth factor- β 1 (TGF- β 1) is initially loaded onto the SF scaffolds by physical absorption, which are then successively functionalized with bone marrow mesenchymal stem cells (BMSCs)-specific-affinity peptide (E7) via gradient degradation coating of Silk fibroin Methacryloyl (SiLMA)/Hyaluronic acid Methacryloyl (HAMA). Such SF-based scaffolds exhibit excellent structural stability and cartilage-like mechanical properties, thus providing a desirable 3D microenvironment for cartilage reconstruction. Furthermore, rapid initial release of E7 during the first few days, followed by slow and sustained release of TGF- β 1 for as long as few weeks, synergistically induced the recruitment of BMSCs and chondrogenic differentiation of them in vitro. Finally, in vivo studies indicate that the implantation of the biofunctional scaffold markedly promote in situ cartilage regeneration in a rabbit cartilage defect model. It is believed that this cartilage-biomimetic biofunctional SF-based scaffold with sequential controlled release of E7 and TGF- β 1 may have a promising potential for improved cartilage tissue engineering.

1. Introduction

Articular cartilage (AC) injury is a common orthopedic disease in clinics.^[1] AC is a specialized connective tissue with superior biomechanical properties such as high resilience and deformability; however, as an avascular and aneural tissue, the degenerative AC lacks the capability to self-heal after damage.^[2–4] Current treatments for cartilage defects include marrow stimulation, autografting, and matrix-induced autologous chondrocyte implantation, but these treatments are in most cases only for symptom relief and do not ensure the regeneration of functional cartilage for a complete, long-term recovery of the joint.^[5–8] Therefore, how to effectively treat AC injury has always been an important problem in clinical medicine.

In recent years, a promising solution to this problem that has received considerable attention is one that realizes one-step in situ cartilage repair by integrating endogenous bone marrow mesenchymal stem cells (BMSCs) with suitable biological

Z. Mao, S. Wu, J. Guan
International Research Center for Advanced Structural and Biomaterials
School of Materials Science & Engineering
Beihang University
Beijing 100191, China
E-mail: wusj@buaa.edu.cn; juan.guan@buaa.edu.cn

Z. Mao, Y. Zheng
School of Materials Science and Engineering
Peking University
Beijing 100871, China

X. Bi
Key Laboratory for Biomechanics and Mechanobiology of Ministry of Education
School of Biological Science and Medical Engineering
Beihang University
Beijing 100083, China

X. Bi, J. Guan
Beijing Advanced Innovation Center for Biomedical Engineering
Beihang University
Beijing 100083, China

C. Wu, X. Shu
Beijing Jishuitan Hospital
Beijing Research Institute of Orthopedics and Traumatology
Beijing 100035, China
E-mail: shuxiong@jst-hosp.com.cn

R. O. Ritchie
Department of Materials Science and Engineering
University of California
Berkeley, CA 94720, USA

The ORCID identification number(s) for the author(s) of this article can be found under <https://doi.org/10.1002/adhm.202201588>

DOI: 10.1002/adhm.202201588

materials.^[9–11] The key to this cell-free strategy is to build an ideal biofunctional scaffold. The scaffold should not only have suitable mechanical properties and micrometer-sized porous morphology, but also have the ability to maintain such mechanical and structural stability in vivo to permit the infiltration of cells and the ingrowth of new tissue.^[12,13] At the same time, the scaffold ideally should recruit sufficient endogenous stem cells (MSCs) to the injured area to promote chondrogenic differentiation of MSCs, thereby avoiding operational, cost, and regulatory issues associated with cell manipulation.^[14,15]

Silk fibroin (SF) is a promising biomaterial for the construction of such tissue engineering scaffolds due to its good biocompatibility, nonimmunogenicity, controllable degradation, and excellent mechanical properties.^[16–19] More importantly, the properties of SF scaffolds can be regulated either through self-assembly of β -sheets or/and chemical crosslinking reactions.^[20] In fact, in the case of SF, the chemical crosslinks not only formulate covalent linkages but also promote and regulate the formation of β -sheets, thereby generating a dual-crosslinked network structure to regulate the comprehensive properties of SF scaffolds.^[21] In fact, we have previously developed cryogelled dual-crosslinked SF scaffolds with robust mechanical performance and dynamic fatigue resistance, as well as good BMSCs biocompatibility and histocompatibility for soft tissue engineering.^[22,23]

In addition to biomaterials, bioactive molecules are another key element of endogenous cell recruitment strategies, which endow biomaterials with the functionality to stimulate the recruitment and chondrogenic differentiation of BMSCs for articular cartilage regeneration.^[11] Recently, some studies have shown that a peptide with the sequence EPLQLKM (E7) can modulate and facilitate BMSCs homing.^[9,24] This affinity peptide has been successfully incorporated into different scaffolds to develop a bone marrow-specific homing scaffolding system, and has generated satisfactory results in vitro or in vivo without species specificity.^[25] Ao et al. demonstrated that E7-immobilized SF-gelatin scaffolds could accelerate the cartilage healing rate in a rabbit model, which was mostly attributed to its BMSCs recruitment.^[9] Additionally, it is also important to maintain the chondrogenic microenvironment of migrating BMSCs. Previous studies found that TGF- β 1 as a bioactive factor can reproducibly facilitate BMSCs chondrogenesis; as such, it is now widely used in cartilage tissue engineering.^[26] Chen et al.^[26] showed that the TGF- β 1 factor loaded into SF coatings on gelatin scaffolds could enhance chondrogenic differentiation of BMSCs in vitro and promote cartilage defect repair in vivo. However, these bioactive substances still have some drawbacks, including short half-lives, easy digestion by proteases, rapid diffusion after injection, and inflammatory side effects after bolus injection.^[27] Ideally, an early release of chemoattractant could facilitate cell migration, with the subsequent prolonged release of chondrogenic bioactive factors inducing migratory cells to secrete extracellular matrix (ECM) components.^[28,29] Therefore, it is important to design the sequential and controlled release of bioactive factors in scaffolds to enhance the effect of any drug-mediated in situ cartilage regeneration strategy.

Drugs or bioactive factors are designed to be delivered to the site of damage via covalent binding^[29] and noncovalent absorption of multiple biofactors, i.e., by direct entrapment in the car-

rier material or coating on the carrier material.^[26,30,31] For example, Chen et al.,^[26] utilized a SF coating to load stromal-derived factor-1 α (SDF-1 α) and TGF- β 1 simultaneously, which allowed for the continuous and slow release of factors with the degradation of the SF. Although the SF coating can carry peptide factors and provide sustained release, varied factors cannot be released independently. However, in contrast, the coordinated use of physical absorption and coatings can solve this problem. For example, Hwang et al.,^[31] developed a double-cryogel system composed of gelatin/chitosan cryogel surrounded by gelatin/heparin cryogel for dual drug delivery with different release kinetics. In addition, the coating in this system had the characteristic of gradient degradation to enable more accurate control of the independent release of the two drugs. Until now, numerous studies have investigated drug delivery and release in cartilage regeneration,^[26,30,32] but few have comprehensively focused on the synergistic effect of two drugs released sequentially from a robust and elastic scaffold platform for cartilage tissue regeneration.

In this work, we developed a cell-free functional silk fibroin scaffold for cartilage repair with sequential and controlled release of E7 and TGF- β 1. TGF- β 1 was initially loaded onto the SF cryogel scaffolds by physical adsorption, and E7 was then loaded by physical entrapment in a fast-degradation coating (SilMA/HAMA). In vitro and in vivo studies were designed to show the synergistic effects on the recruitment of BMSCs and directed chondrogenic differentiation from such programmed release of E7 and TGF- β 1. Accordingly, here we are proposing this biomaterial platform functionalized by TGF- β 1 and E7 as a promising new route for improved cartilage regeneration.

2. Results

2.1. Fabrication and Characterization of SF-Based Scaffolds with SilMA/HAMA Coatings

We successfully fabricated a novel SF-based scaffolds with two growth factors loaded separately, namely TGF- β 1 absorbed onto the SF scaffold and E7 in the hydrogel coating (**Figure 1**). The detailed methods are described in the Supporting Information. The preparation of mechanically robust SF cryogel scaffolds can be found also in our earlier studies.^[23] For the preparation of the coating, briefly we first synthesized and characterized Silk fibroin Methacryloyl (SilMA) by methacrylate substitution of the primary amines of SF. As shown in **Figure 2a**, the gelation of SilMA was induced by UV light, with the chemical modification result verified by ¹H-NMR results (**Figure 2b**). Specifically, there was a characteristic resonance of the methacrylate vinyl group (displacement value $\delta = 6.2\text{--}6.0$ and $5.8\text{--}5.6$ ppm) and the methyl group of glycidyl methacrylate (GMA) at $\delta = 1.8$ ppm in the modified SilMA, which indicated the successful addition of the GMA. Next, we synthesized Hyaluronic acid Methacryloyl (HAMA) and mixed with SilMA to formulate a photocurable SilMA/HAMA solution. E7 was introduced into the solution before the UV-induced photo-crosslinking of the hydrogel coating. The chemical structures and reactions are indicated in **Figure 1b**. Coating samples showed Fourier transform infrared spectroscopy (FTIR) spectra, with amide I, II, and III peaks at 1658, 1548, and 1249 cm^{-1} respectively, indicating that α -helix and random coils were the dominant conformation in the SilMA/HAMA (**Figure 2c**).

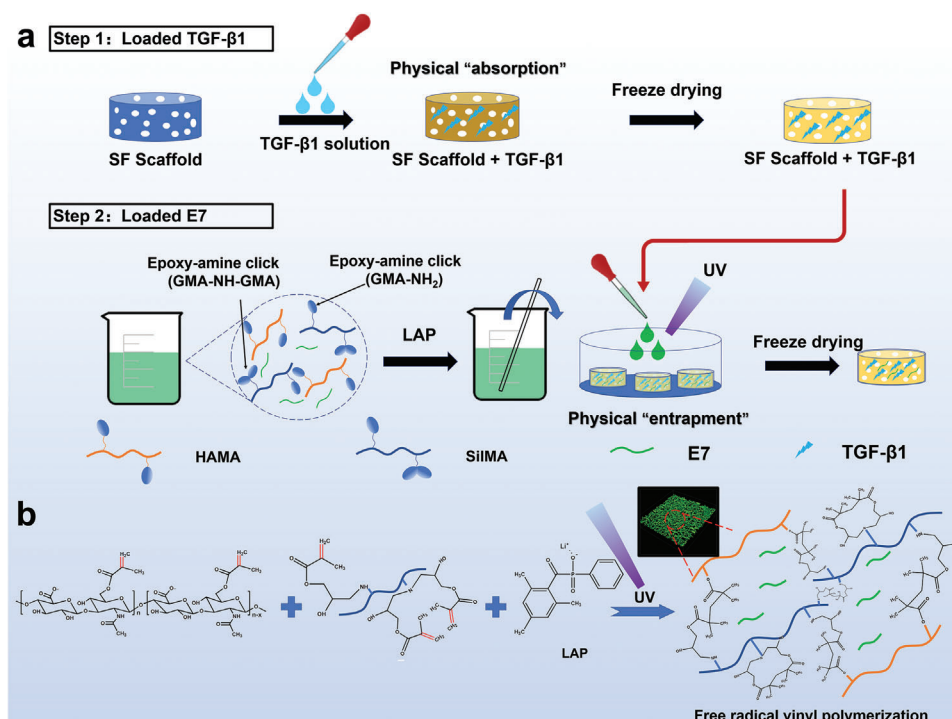


Figure 1. Preparation of biofunctional SF scaffolds. a) Schematic illustrations of the drug-loading processes of TGF- β 1 in the SF scaffold core via physical adsorption and E7 in a SilMA/HAMA coating. b) Structure illustrations of the hydrogel coating and the physical entrapment of E7.

We compared the morphologies of the SF-based scaffolds with/without the SilMA/HAMA coating. The coated SF-based scaffolds exhibited a thin coating in the pore walls and surface layers, but still retained a porous structure (Figure 2d). A water contact angle test was used to analyze the effect of the surface coating on the hydrophilicity of the scaffolds. This showed that the average water contact angle of the SF scaffolds decreased from $\approx 70^\circ$ to $\approx 48^\circ$ with addition of the SilMA/HAMA coating (Figure 2e), due to the hydrophilic nature of HAMA in the coating.

2.2. Mechanical Properties of the SF Scaffolds and SilMA/HAMA-Coated SF Scaffolds

To investigate the comprehensive mechanical properties of the SilMA/HAMA-coated SF scaffolds, we carried out uniaxial tension and compression testing. The tensile stress–strain curves in Figure 2f,g showed that the tensile strength and modulus of the SilMA/HAMA-coated SF scaffolds were generally higher than that in the SF scaffolds; specifically the tensile strength increased from 217.3 ± 12.5 to 300.6 ± 19.0 kPa, respectively, with a tensile modulus increase from 174.5 ± 8.1 to 367.6 ± 7.6 kPa. However, the tensile breaking strain of the SilMA/HAMA-coated SF scaffolds was lower than that of the SF scaffolds. Specifically, the respective values of these tensile breaking strains of the SF scaffolds and SilMA/HAMA-coated SF scaffolds were $420.6 \pm 9.2\%$ and $195.1 \pm 10.4\%$. Importantly, the SilMA/HAMA-coated SF scaffolds still maintained high breaking strains in the wet state. With respect to the compressive behavior, the compression modulus of the SilMA/HAMA-coated SF scaffolds also increased

from 42.3 ± 6.6 to 101.3 ± 8.0 kPa after adding the coating. Typical compressive stress–strain curves and the compression modulus results are shown in Figure 2i,j.

We further examined the fatigue resistance using cyclic tensile and compression tests on the SilMA/HAMA-coated SF scaffolds. The cyclic tensile/compressive behavior of the SF scaffolds were characterized in a previous study.^[23] Here, we report only the results for the SilMA/HAMA-coated SF scaffolds. Figure 2h,k revealed that both the SF scaffolds and SilMA/HAMA-coated SF scaffolds can maintain structural integrity and high elasticity over 1000 cycles of tensile and compression loading/unloading. These results demonstrate that the SilMA/HAMA coating can enhance the strength and modulus of the SF scaffolds without compromise to their recoverability and elasticity.

2.3. Sequential Drug Release of SF Scaffolds with E7 and TGF- β 1

The sequential and sustained release of drugs is critical for the strategy of endogenous cell recruitment for AC regeneration.^[11] Therefore, we designed a double-drug system composed of TGF- β 1 loaded in the SF scaffold core and E7 loaded in the SilMA/HAMA-coating. E7 was released initially on the degradation/decomposition of the coating, with TGF- β 1 released in a sustained manner from the core scaffold in vitro and in vivo (Figure 3). To reveal the dual release behavior, we first studied the decomposition of the SilMA/HAMA coating. SilMA/HAMA samples experienced about 50% mass loss within 24 h (Figure 3a), mainly due to the rapid decomposition of the HAMA. After 24 h, this rate slowed down until the 14th day; the remaining sample

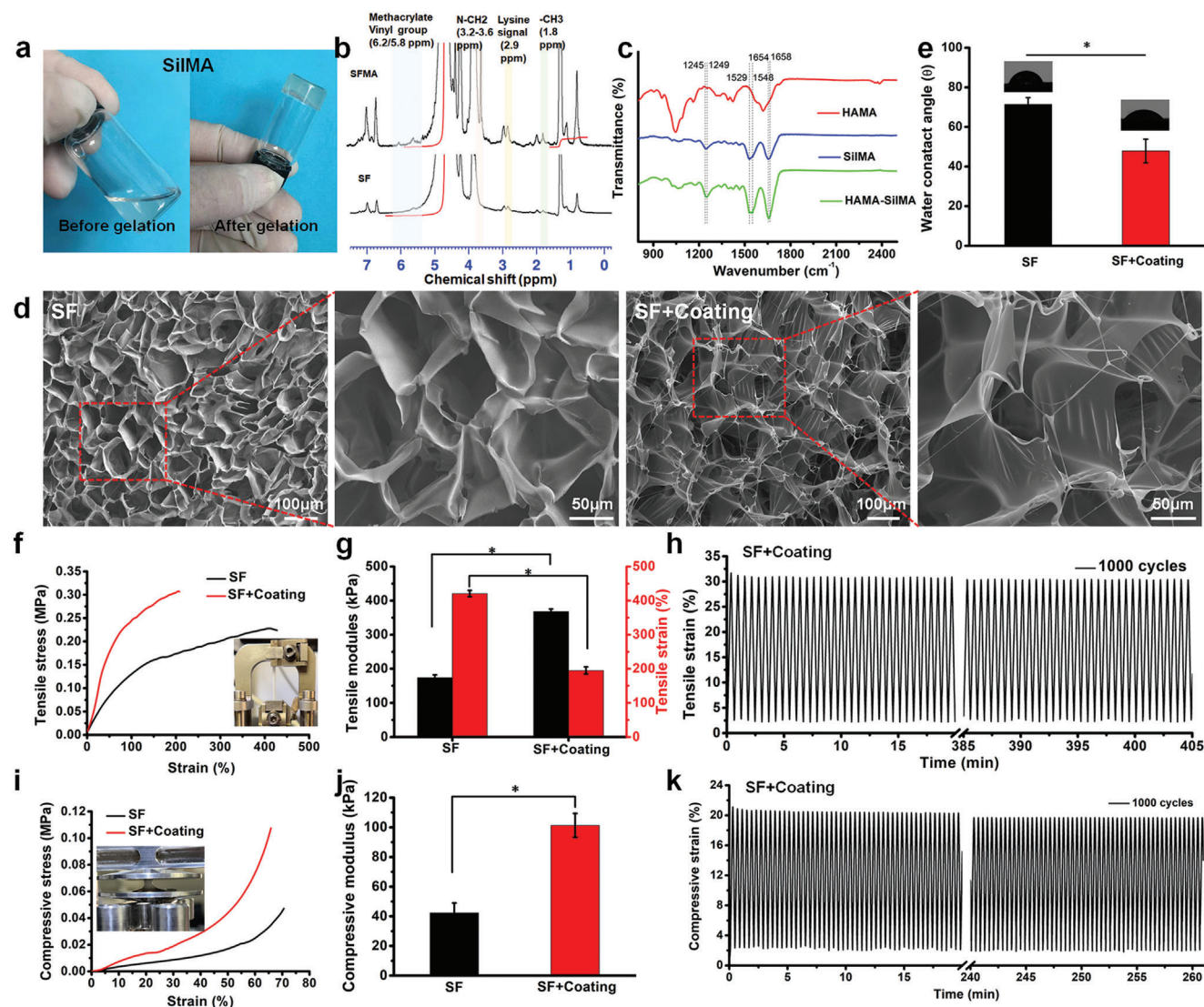


Figure 2. Fabrication and characterization of SF-based scaffolds with a SiIMA/HAMA coating. a) Photographs of the SiIMA before and after gelation. b) ^1H -NMR spectra of the SF and amine-substituted SiIMA. c) FTIR spectra of the HAMA, SiIMA and HAMA/SiIMA. d) Representative scanning electron microscopy (SEM) images of the SF scaffolds and SiIMA/HAMA-coated SF scaffolds. e) Water contact angles on the SF scaffolds and SiIMA/HAMA-coated SF scaffolds. f) Representative engineering tensile stress–strain curves and g) tensile modulus and breaking strains of the SF scaffolds and SiIMA/HAMA-coated SF scaffolds. h) The tensile fatigue behavior of the SiIMA/HAMA-coated SF scaffolds. i) Representative compressive stress–strain curves and j) compressive modulus of the SF scaffolds and SiIMA/HAMA-coated SF scaffolds. k) Compressive fatigue behavior of the SiIMA/HAMA-coated SF scaffolds. Data are presented as means \pm SD, $n = 3$, $*p < 0.05$.

mass at this juncture was $\approx 30\%$, mainly due now to the SiIMA residue in the coating. This suggests that SiIMA/HAMA materials can usefully exhibit graded degradation characteristics after implantation.

Next, we compared the release behavior of TGF- $\beta 1$ with and without the SiIMA/HAMA coating on the SF scaffolds. Quantitative analysis of the release of TGF- $\beta 1$ from SF scaffolds in vitro was obtained using Enzyme Linked Immunosorbent Assay (ELISA) kits. In the absence of the SiIMA/HAMA coating, a total of $\approx 80\%$ of the TGF- $\beta 1$ was released after 14 days of immersion in phosphate buffer saline (PBS) solution; with the coating applied, only $\approx 60\%$ of the TGF- $\beta 1$ was released (Figure 3b). These results demonstrated that the presence of the SiIMA/HAMA coat-

ing result in a more sustained release of TGF- $\beta 1$ than with simple physical adsorption in uncoated SF scaffolds.

In vitro and in vivo release of the E7 that was loaded into the coating of the SF scaffolds through physical adsorption was investigated using confocal laser scanning microscopy (CLSM) and an in vivo imaging system (IVIS) (Figure 3c,e); this was compared with direct loading in the absence of a coating. The attenuation of the fluorescence intensity of Fluorescein Isothiocyanate (FITC)-labeled E7 in the SF scaffold was analyzed corresponding to the release of the E7. E7 was loaded into the crosslinked structure of the coating during the free radical polymerization between SiIMA and HAMA. The loaded SF scaffolds were incubated in a PBS buffer at 37°C for 7 days. For direct adsorption into the SF

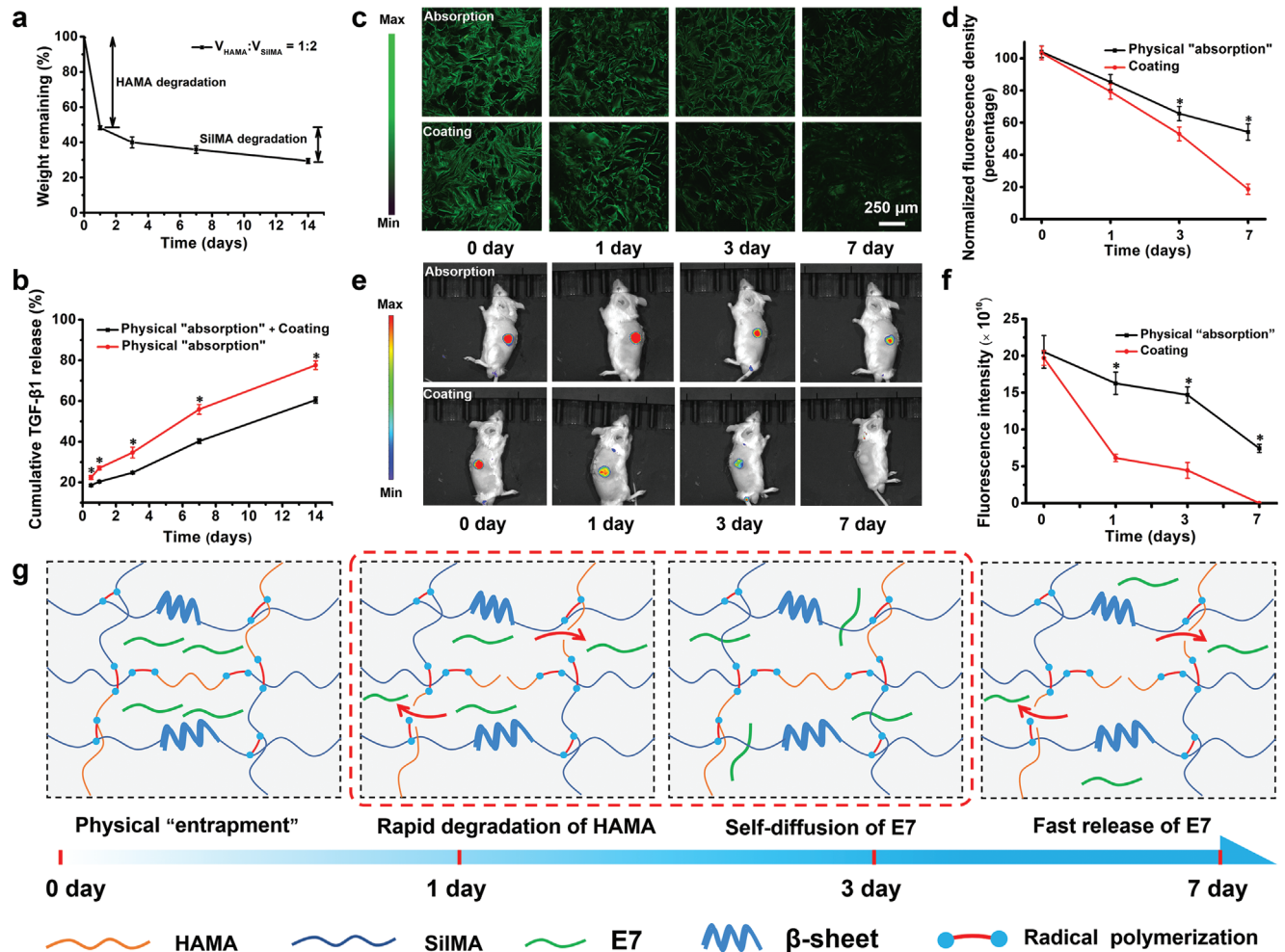


Figure 3. Evaluation of the double drug release system of SF scaffolds in vitro and in vivo. a) The enzymatic degradation behavior of the SiMA/HAMA coating in protease solution. b) The cumulative TGF- β 1 release behavior from the SF scaffolds via direct physical adsorption and physical adsorption in the SiMA/HAMA coating. c) Representative CLSM images of FITC-labeled E7 (green) on the SF scaffolds via direct adsorption and SiMA/HAMA coating adsorption at various time points. d) Quantitative fluorescence intensity of E7 on the SF scaffolds at various time points. e) High-sensitivity in vivo imaging of the fluorescence of the FITC-labeled E7 SF scaffolds at various time points after subcutaneous implantation in Balb/c mice. f) Quantitative fluorescence intensity of FITC-labeled E7 in vivo at various time points. g) Schematic illustrations of the structure changes induced by E7 release after implantation in vivo. Data are presented as means \pm SD, $n = 3$, $*p < 0.05$.

scaffold, the fluorescence intensity of E7 declined to 40% of the initial value after 7 days of incubation (Figure 3d). For the group with the SiMA/HAMA coating, the fluorescence intensity was $\approx 20\%$ of the initial value after 7 days of incubation, indicating a significantly faster release (Figure 3e). With respect to in vivo imaging in live mice (Figure 3f), the fluorescence intensity of E7 loaded by the SiMA/HAMA coating was observed to decrease quickly and was effectively reduced to zero after 7 days of implantation, indicating that most of the E7 had been released. However, the E7 adsorbed in the scaffolds displayed a slower release rate at all measured time points, actually in a manner that is consistent with the in vitro results. In light of these results, it is evident that the process of loading in the coating is highly beneficial for the fast initial release of E7 within a week after implantation. The mechanism of controlled release of E7 is illustrated in Figure 3g. This clearly contributes to better stem cell recruitment at the initial stage. Due to its high cost, the experiment to show the

release behavior of TGF- β 1 in vitro was not conducted. However, it can be assumed that the release of TGF- β 1 loaded by physical adsorption in SF scaffolds is controlled by the degradation of the SF scaffold core. Therefore, the release data of physically adsorbed E7 in the SF scaffold may be an estimate of the release data of TGF- β 1 from the SF-TGF- β 1-E7 scaffolds.

2.4. In Vitro Adhesion, Recruitment, Proliferation, and Chondrogenic Differentiation of BMSCs on SF Scaffolds with Drug Loadings

In vitro BMSCs affinity to the SF scaffolds was performed with a cell attachment assay. After 7 days incubation with rat bone marrow mesenchymal stem cells (rBMSCs), cytoskeleton staining, and Live/Dead staining revealed that the rBMSCs had good attachment and had spread over all the SF scaffolds with high cell

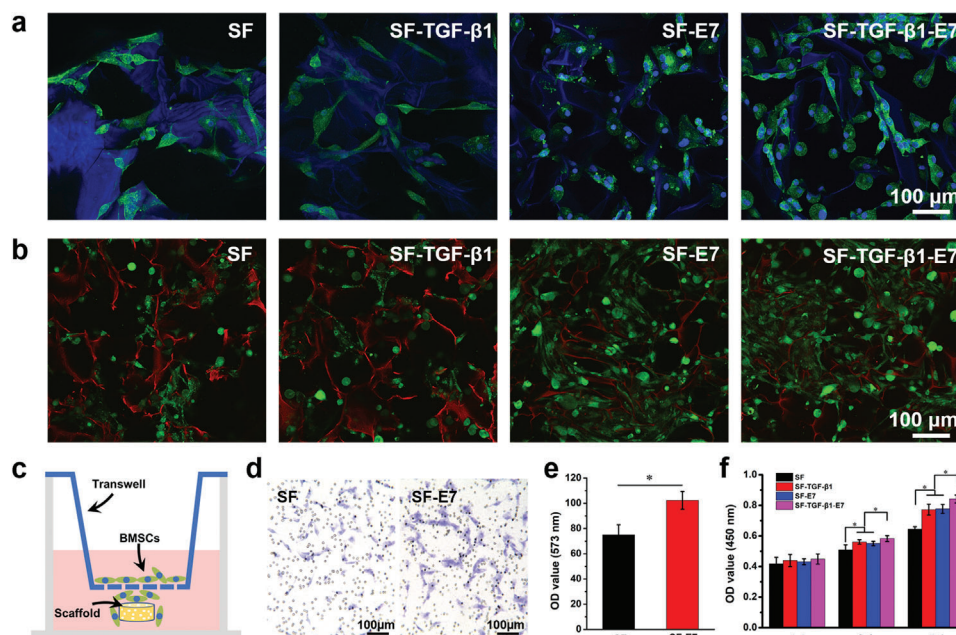


Figure 4. In vitro biological assessments on SF scaffolds with varied loadings of TGF- β 1, E7, and TGF- β 1+E7 and stem cells recruitment by SF scaffolds with or without loadings of E7. a) Confocal images of rBMSCs on SF scaffolds cultured for 7 days. b) Live/Dead cell viability (green: live cells, red: dead cells/scaffold) of rBMSCs on SF scaffolds cultured for 7 days. c) Schematic depiction of the Transwell assay in studying rBMSCs migration to SF and SF-E7 scaffolds. d) Optical microscope images of the rBMSCs-laden SF and SF-E7 scaffolds for 12 h by dissolving crystal violet. e) Quantification of migrated rBMSCs to various scaffolds, as determined by spectrophotometrically at 573 nm. f) CCK-8 assays on cell proliferation performed after 1, 3, and 7 days of cell culture. Data are presented as means \pm SD, $n = 3$, $*p < 0.05$.

viability (Figure 4a,b). Specifically, a significantly greater number of cells were adhered into the drug-loaded SF-E7 scaffolds and SF-TGF- β 1-E7 scaffolds compared to the SF scaffolds and SF-TGF- β 1 scaffolds, demonstrating the BMSCs attachment capability of the E7 peptide.^[9] To directly demonstrate the MSCs-homing capability, the Transwell assay using rBMSCs was conducted on the SF and SF-E7 scaffolds (Figure 4c). As shown in Figure 4d,e, compared to the SF scaffolds, the SF-E7 scaffolds were found to induce greater MSCs migration and provided directional migration or homing of the rBMSCs.

Additionally, the CCK-8 assay showed that both TGF- β 1 and E7 are important to mediate the proliferation of rBMSCs on the SF scaffolds (Figure 4f). The optical density (OD) values of the three drug-loaded SF scaffolds were significantly higher than that of the control group of pure SF scaffolds at each recorded time point. Additionally, the proliferation of the SF-TGF- β 1-E7 scaffolds was the larger, which indicates the synergistic role of TGF- β 1 and E7 in promoting cell adhesion and growth.

The chondrogenesis of rBMSCs grown on the surfaces of the SF scaffolds was further evaluated by quantitative reverse transcription polymerase chain reaction (qRT-PCR) (Figure 5a–d). The expressions of the chondrogenic genes (Aggrecan, Sox 9, and COL 2) were compared. The SF-TGF- β 1 scaffolds and SF-TGF- β 1-E7 scaffolds showed significantly higher expression than the SF scaffolds and SF-E7 scaffolds after 7 and 14 days of chondrogenic induction. In particular, the messenger Ribonucleic Acid (mRNA) levels of Sox9, COL 2, and aggrecan of BMSCs on SF-TGF- β 1-E7 scaffolds were, respectively, factors of 9.4, 3.4, and 5.0 higher than those on the SF scaffolds after 14 days of culture; additionally, the COL 1 level of the SF-TGF- β 1-E7 scaffolds was

higher than that of other groups after 14 days of culture. Moreover, the COL 2/COL 1 ratio of the SF-TGF- β 1-E7 scaffolds was also higher than that on other groups (Figure 5e). Subsequently, Western Blot analysis was conducted to detect the levels of chondrogenic proteins expressed by rBMSCs on the SF and SF-TGF- β 1-E7 scaffolds (Figure 5f). After 2 weeks of incubation, the expression of the COL 2, aggrecan, and Sox 9 proteins in rBMSCs on SF-TGF- β 1-E7 scaffolds was higher than that on SF scaffolds.

To further analyze the chondrogenic capacity of different SF scaffolds in vitro, histological and immunohistochemical analysis of the resultant tissue was performed. We seeded cell suspensions on the scaffolds for cartilage tissue formation. The results in Figure 5g showed a general trend of increasing chondrogenic tissue formation from 14 to 21 days, with the deeper staining of SF-TGF- β 1-E7 scaffolds indicating faster extracellular matrix formation. From the H&E staining results (Figure 5g), compared with SF scaffolds, the SF-TGF- β 1-E7 scaffolds had greater cell density at 14 and 21 days, with the pores filled with more cells and matrices. Safranin O and Alcian blue staining in the 2nd and 3rd columns in Figure 5g showed that the SF-TGF- β 1-E7 group formed larger contents of glycosaminoglycan and sulfated proteoglycan than the SF group at both 14 and 21 days. To verify the types of newly formed cartilage, we investigated the expression of type I collagen (COL 1), type II collagen (COL 2), and aggrecan by immunohistochemistry corresponding to the right three columns (Figure 5g). At 14 and 21 days, the expression of COL 1 as a major collagen in fibrocartilage was higher in the SF group than in the SF-TGF- β 1-E7 group. In contrast, the expressions of COL 2 and aggrecan were higher in the SF-TGF- β 1-E7 group than in the SF group at 14 and 21 days.

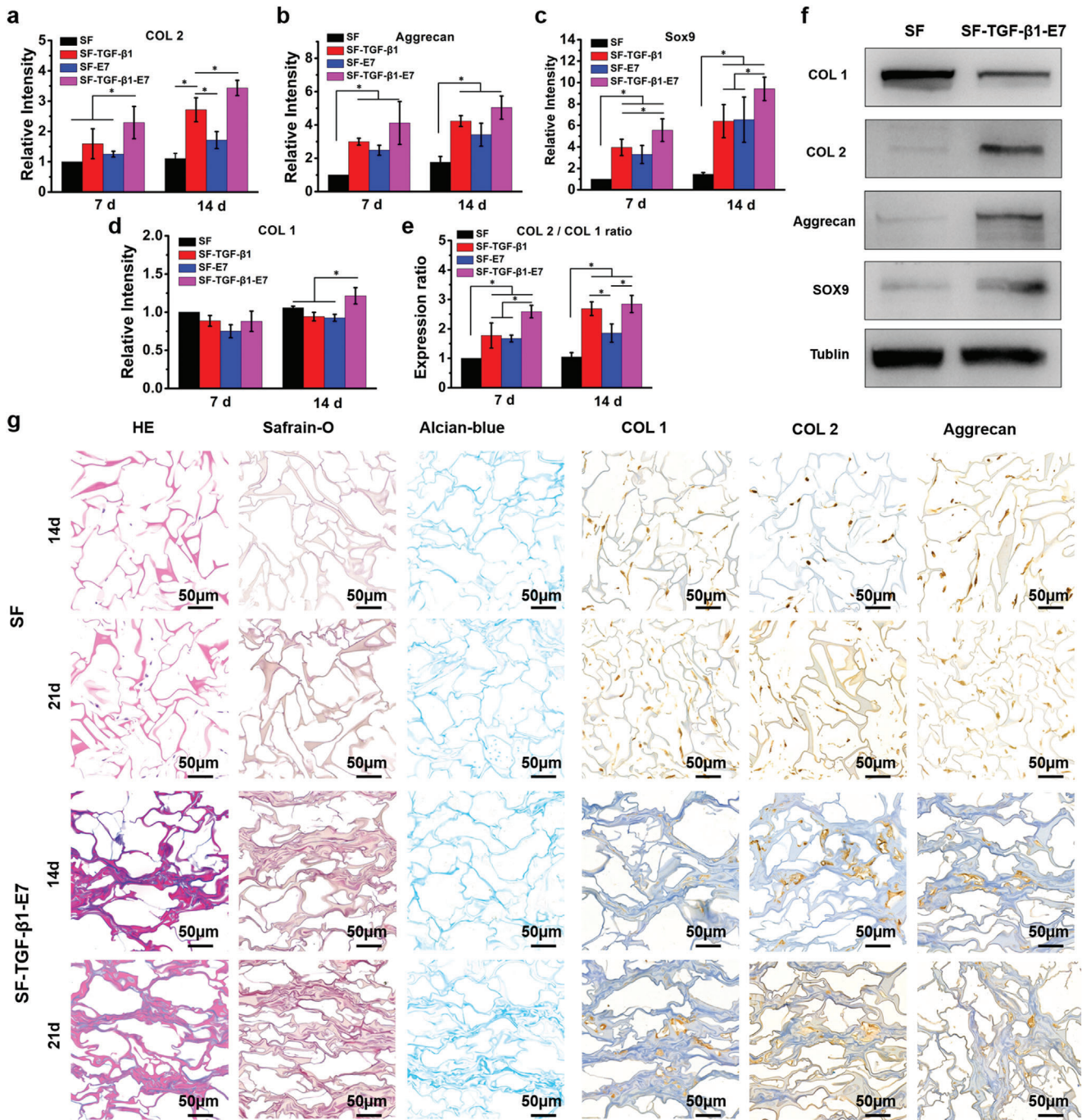


Figure 5. In vitro chondrogenic differentiation of BMSCs on SF scaffolds with varied drug loadings. a–c) RT-qPCR analysis of the expression of chondrogenic differentiation genes (COL 2, Aggrecan, and Sox9) and d) osteogenic gene (COL 1). e) The COL 2/COL 1 ratio of various SF scaffolds. f) Western Blot results of chondrogenetic proteins of rBMSCs on scaffolds after 14 days of culture. g) Evaluation of in vitro cartilage formation at the SF and SF-TGF-β1-E7 scaffolds after 14 and 21 days of rBMSCs culture. Data are presented as means ± SD, $n = 3$, $*p < 0.05$.

2.5. In Vivo BMSCs Recruitment of SF Scaffolds and General Evaluation of the Repaired Knees

To investigate the BMSCs homing capacity of the SF scaffolds with E7 in vivo, these SF-E7 scaffolds were implanted into the defected knee joint of a rabbit via a standard operation procedure

(Figure 6a). 1 week after implantation, the SF-E7 scaffolds displayed a more abundant and denser filling of cells in the defect than the SF scaffolds (Figure 6b,c). Although these cells were not proven to be MSCs in Figure 6b, we could deduce from previous studies that the main cell source during the first week of implantation was BMSC in vivo using similar microfracture method

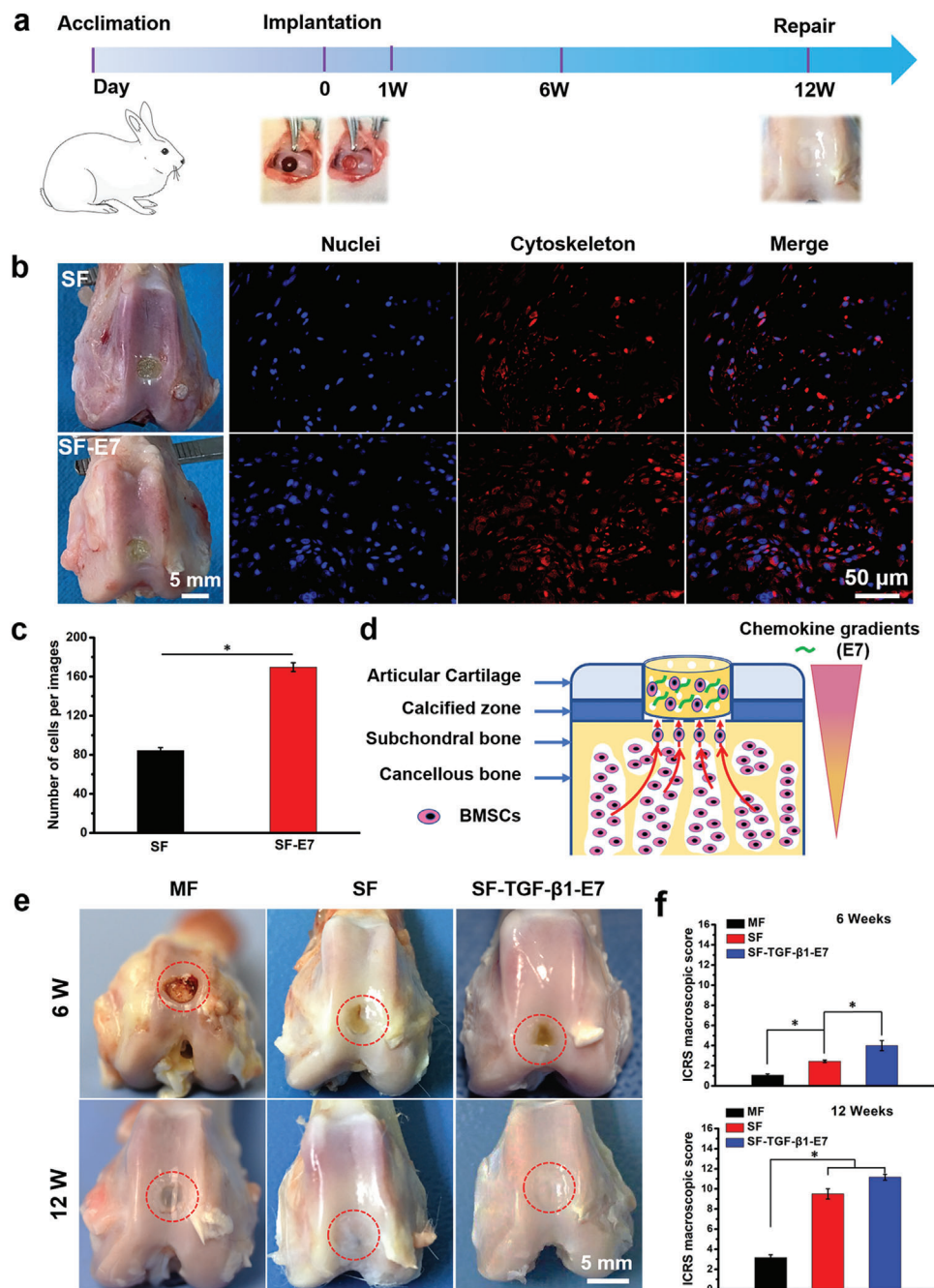


Figure 6. Animal experimental design and macroscopic assessment of in vivo cartilage repair. a) Overall experimental design based on a rabbit cartilage defect model. b) Photo images and CLSM images of BMSCs recruitment of SF and SF-E7 scaffolds 1 week after implantation on a rabbit knee-defect model. c) Comparison of cell numbers infiltrated into the SF and SF-E7 scaffolds. d) Schematic representation of BMSCs migration and recruitment in response to the E7 induced chemokine gradients. e) Representative macroscopic images of repaired tissues at 6 and 12 weeks postoperation. The red circle indicates the defect sites. f) ICRS macroscopic scores from the macroscopic images. Data are presented as means \pm SD, $n = 3$, $*p < 0.05$.

to create cartilage defects.^[33,34] Therefore, these results provided strong evidence that the E7 peptide can promote the migration of more BMSCs by inducing in vivo chemokine gradients around the cartilage defect (Figure 6d).

The effects of cartilage repair after 6–12 weeks in vivo are compared for the various SF scaffolds in Figure 6a–e. After 6 weeks of scaffold implantation, gross observations revealed that cartilage

defect was barely filled with new cartilage in the control group (Microfracture, MF), whereas the defects in the SF and SF-TGF- β 1-E7 groups were partially refilled. After 12 weeks implantation, improved repaired tissues and integrations were observed in all groups compared with those at 6 weeks. However, the integration with the surrounding normal cartilage were distinct. The defect in the MF group was grown with uneven tissue with an obvious

void. The SF-TGF- β 1-E7 groups displayed the best performance among all the groups, with a complete and smooth macroscopic appearance and better integration with the surrounding cartilage.

It should be noted that the International Cartilage Repair Society (ICRS) macroscopic score was the highest for the SF-TGF- β 1-E7 group at both 6 weeks (4.0 ± 0.5) and 12 weeks (11.1 ± 0.2) after implantation (Figure 6f). Based on such ICRS scores to provide an assessment of overall cartilage repair, the repaired/grown cartilage for the SF-TGF- β 1-E7 group could be considered as nearly normal (grade II). Surprisingly, an almost equal score as that for the SF-TGF- β 1-E7 group was achieved for the SF group at 12 weeks after implantation. Thus, a more comprehensive evaluation still needs to be conducted to discern specific and detailed differences.

2.6. Histological and Immunological Assessment of Repaired Tissue

The histological and immunological assessment of repaired tissues was additionally carried out. The regional magnified images from hematoxylin and eosin (H&E) staining are shown in Figure 7. At 6 weeks after surgery, the defect in the MF group was partly filled with disordered tissue in contrast to the host cartilage. For the SF and SF-TGF- β 1-E7 groups, more highly organized chondrocyte-like cells were observed, and cartilage-like tissue ingrowth appeared within the scaffolds. However, the boundary between the new and normal cartilage was apparent in each group. At 12 weeks after surgery, the defect in the SF and SF-TGF- β 1-E7 scaffolds was completely repaired with new cartilage tissue. Moreover, typical chondrocytes were arranged in columns or clusters and the surface was as smooth as the surrounding host cartilage; the boundary between the repaired tissue and normal cartilage was now obscured.

Toluidine blue (TB) staining and Safranin O/Fast Green staining was further performed to detect the distribution of proteoglycans and glycosaminoglycan (GAG) in the regenerated tissue (Figure 7). The repaired tissue for the SF-TGF- β 1-E7 group displayed strong positive staining with TB and Safranin O/Fast Green than with MF and SF groups at both 6 and 12 weeks after implantation, indicating a rich GAG deposition and newly formed cartilage. Additionally, Sirius red staining and immunohistochemical staining was further used to analyze the deposition and organization of the collagen II (COL 2) in the regenerated tissues of all groups. As shown in Figure 7a; and Figure S1 (Supporting Information), there were more chondrocytes and a higher content of COL 2 in the SF-TGF- β 1-E7 group at 12 weeks after surgery than in the other two groups at both the surface and central areas. These results clearly indicate that the SF-TGF- β 1-E7 group exhibited the best performance for chondrogenic differentiation and COL 2 deposition of the recruited BMSCs. In contrast, the autogenic cartilage repair for the MF group resulted in only disordered growth of fibrocartilage and fibrous tissue.

3. Discussion

The repair of articular cartilage injury remains a major clinical challenge due to the poor self-healing capacity of cartilage

tissue.^[1] In recent years, the endogenous cell recruitment strategy for in situ tissue regeneration has proven to be superior to the exogenous cell implantation strategy.^[35,36] Our strategy in this work was to construct a biofunctional scaffold that can effectively and specifically recruit endogenous stem cells to the site of injury and improve the local chondrogenic microenvironment. The objective was to take advantage of the body's own regenerative potential to achieve in situ AC regeneration.^[9,29,37]

The developed novel biomimetic SF scaffolds loaded with two growth factors, E7 in the coating and TGF- β 1 absorbed at the core of SF scaffolds, were found to achieve a sequential and controlled release of two biofactors and to exert functions of stem cell homing and chondrogenic induction. We revealed that naturally occurring cell migration was not sufficient within the limited time window (1 day) after cartilage injury.^[11] We showed that E7 loaded within a photocured SilMA-HAMA coating on the SF scaffolds could be released faster than the direct loading in the SF scaffolds, leading to more effective BMSCs recruitment. The initial release profiles of E7 from the SF scaffolds were demonstrated and confirmed using CLSM and an in vivo imaging system (IVIS) (Figure 3d–f). Cytoskeleton, Live/Dead and Transwell-migration assay in vitro analyses showed that E7 had significantly promoted adhesion and recruitment of the BMSCs (Figure 4a–e).

In addition, the application of such coatings did not affect the porosity of the SF scaffolds, which could provide infiltration channels for dissociative or migratory stem cells, transport cell nutrients, and facilitate waste discharge.^[25,38] More importantly, the incorporation of the SilMA-HAMA coatings on the SF scaffolds significantly increased their hydrophilicity and improved the ECM microenvironment.^[39]

We also found that a sustained release of TGF- β 1 was achieved through gradual degradation of the SilMA-HAMA coating and gradual diffusion from the scaffold core, leading to chondrogenic differentiation of BMSCs which aided the initiation of cartilage formation. Such a controlled slow release of TGF- β 1 can act to prevent synovial fibrosis and endochondral ossification.^[40,41] Our results on the in vitro chondrogenic performance agreed well with previous studies,^[26,42,43] demonstrating the ability of TGF- β 1 to promote chondrogenic differentiation of BMSCs and to provide a good chondrogenic environment. It was also demonstrated that TGF- β 1 and E7 engage synergistically to promote cartilage regeneration.

Under physiological conditions, articular cartilage was subjected to repeated and dynamic mechanical stimulations, which require the scaffold implant to be resistant to specific cyclic fatigue.^[44] In our earlier study,^[22,23] SF scaffolds with dual-crosslinked structures exhibited superior tensile strength and compressive strength than freeze-dried SF scaffolds. Here the strengths of the SilMA-HAMA coated SF scaffolds were substantially further improved. Moreover, the soft, elastic and fatigue-resistant properties of the SilMA-HAMA coated SF scaffolds were maintained. As studies have shown that dynamic mechanical stimulations generated by proper exercise are conducive to the secretion and efficient flow of synovial fluids, which promote the synthesis of proteoglycan,^[45–48] we strongly believe that the SF scaffolds developed in this study can serve as an in vivo biomimetic platform to withstand dynamic loading and to emulate the chondrogenic microenvironment in the defect.

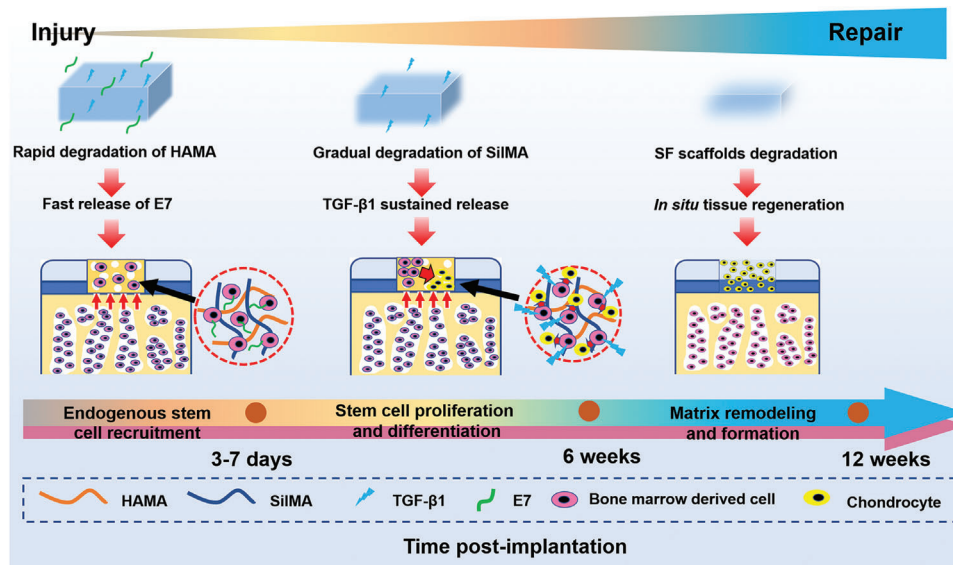


Figure 8. Schematic illustrations of the proposed mechanistic progression of cartilage healing.

load-bearing site, this does not give full play to the mechanical characteristics of the SF scaffolds. In light of this, in future studies the cartilage defect model will need to be further optimized.

4. Conclusion

In this study, we developed a novel silk fibroin scaffold platform with independent controlled release of E7 and TGF- β 1 bioactive substances for cartilage repair. E7 was utilized as a BMSCs homing factor, and TGF- β 1 was selected to direct chondrogenic differentiation of BMSCs. The loading methods of E7 in the photo-crosslinked SiIMA/HAMA coating and TGF- β 1 in the SF scaffold core successfully realized sequential and controlled release of the two biofactors. In vitro BMSCs assessments demonstrated good recruitment ability of endogenous BMSCs and chondrogenic gene expressions for the SF-TGF- β 1-E7 scaffolds. In vivo analysis based on a rabbit knee defect model indicated that the implantation of the SF-TGF- β 1-E7 scaffolds markedly promoted in situ cartilage regeneration. Such a strategy of using cell-free silk fibroin-based biofunctional scaffolds with sequential and controlled releases of E7 and TGF- β 1 provides a promising means for substantially improving in situ cartilage regeneration that can provide new insights into clinical treatments of cartilage defects.

Supporting Information

Supporting Information is available from the Wiley Online Library or from the author.

Acknowledgements

Z.N.M. and X.W.B. contributed equally to this work. This work was financially supported by The National Key R&D Program of China (Grant Nos.

2022YFB3804400, 2018YFA0703100), Beijing Municipal Health Commission (Grant Nos. BMHC-2019-9, BMHC-2021-6, and BJRITO-RDP-2023). The Fundamental Research Fund for Central Universities (Beihang University) is also acknowledged. ROR was supported by the H.T. & Jessie Chua Distinguished Professorship at the University of California Berkeley. All animal experiments were approved by animal care and use committee of Beihang University, Beijing 100083, China and Beijing Jishuitan Hospital, Beijing, 100035, China (approval number 202110-02).

Conflict of Interest

The authors declare no conflict of interest.

Data Availability Statement

The data that support the findings of this study are available in the Supporting Information of this article.

Keywords

BMSC-affinity peptide, controlled release, hyaluronic acid, in situ cartilage repair, silk fibroin, TGF- β 1

Received: June 30, 2022
Revised: October 11, 2022
Published online: November 7, 2022

- [1] Y. Krishnan, A. J. Grodzinsky, *Matrix Biol.* **2018**, *71*, 51.
- [2] C. Qi, J. Liu, Y. Jin, L. M. Xu, G. B. Wang, Z. Wang, L. Wang, *Biomaterials* **2018**, *163*, 89.
- [3] D. J. Huey, J. C. Hu, K. A. Athanasiou, *Science* **2012**, *338*, 917.
- [4] B. J. Huang, J. C. Hu, K. A. Athanasiou, *Biomaterials* **2016**, *98*, 1.
- [5] E. A. Makris, A. H. Gomoll, K. N. Malizos, J. C. Hu, K. A. Athanasiou, *Nat. Rev. Rheumatol.* **2015**, *11*, 21.

- [6] B. Ma, J. C. Leijten, L. Wu, M. Kip, C. A. van Blitterswijk, J. N. Post, M. Karperien, *Osteoarthritis Cartilage* **2013**, *21*, 599.
- [7] J. L. Cook, A. H. Gomoll, J. Farr, *J. Orthop. Res.* **2016**, *34*, 557.
- [8] T. M. Simon, D. W. Jackson, *Sports Med. Arthrosc. Rev.* **2018**, *26*, 31.
- [9] W. Shi, M. Sun, X. Hu, B. Ren, J. Cheng, C. Li, X. Duan, X. Fu, J. Zhang, H. Chen, Y. Ao, *Adv. Mater.* **2017**, *29*, 1701189.
- [10] X. Sun, H. Yin, Y. Wang, J. Lu, X. Shen, C. Lu, H. Tang, H. Meng, S. Yang, W. Yu, Y. Zhu, Q. Guo, A. Wang, W. Xu, S. Liu, S. Lu, X. Wang, J. Peng, *ACS Appl. Mater. Interfaces* **2018**, *10*, 38715.
- [11] Z. Yang, H. Li, Z. Yuan, L. Fu, S. Jiang, C. Gao, F. Wang, K. Zha, G. Tian, Z. Q. Sun, B. Huang, F. Wei, F. Y. Cao, X. Sui, J. Peng, S. B. Lu, W. M. Guo, S. Y. Liu, Q. Y. Guo, *Acta Biomater.* **2020**, *114*, 31.
- [12] Q. Li, S. Xu, Q. Feng, Q. Dai, L. Yao, Y. Zhang, H. Gao, H. Dong, D. Chen, X. Cao, *Bioact. Mater.* **2021**, *6*, 3396.
- [13] K. C. Hung, C. S. Tseng, L. G. Dai, S. H. Hsu, *Biomaterials* **2016**, *83*, 156.
- [14] I. K. Ko, S. J. Lee, A. Atala, J. J. Yoo, *Exp. Mol. Med.* **2013**, *45*, e57.
- [15] D. A. Grande, N. A. Sgallione, *Nat. Rev. Rheumatol.* **2010**, *6*, 677.
- [16] N. Fazal, N. Latief, *Osteoarthr Cartilage* **2018**, *26*, 1583.
- [17] S. Yodmuang, S. L. McNamara, A. B. Nover, B. B. Mandal, M. Aganwal, T. A. N. Kelly, P. H. G. Chao, C. Hung, D. L. Kaplan, G. Vunjak-Novakovic, *Acta Biomater.* **2015**, *11*, 27.
- [18] V. P. Ribeiro, S. Pina, J. B. Costa, I. F. Cengiz, L. Garcia-Fernandez, M. D. M. Fernandez-Gutierrez, O. C. Paiva, A. L. Oliveira, J. San-Roman, J. M. Oliveira, R. L. Reis, *ACS Appl. Mater. Interfaces* **2019**, *11*, 3781.
- [19] Y. Wang, D. D. Rudym, A. Walsh, L. Abrahamsen, H. J. Kim, H. S. Kim, C. Kirker-Head, D. L. Kaplan, *Biomaterials* **2008**, *29*, 3415.
- [20] Y. Zhao, Z. S. Zhu, J. Guan, S. J. Wu, *Acta Biomater.* **2021**, *125*, 57.
- [21] I. Karakutuk, F. Ak, O. Okay, *Biomacromolecules* **2012**, *13*, 1122.
- [22] Z. Mao, X. Bi, F. Ye, X. Shu, L. Sun, J. Guan, R. O. Ritchie, S. Wu, *ACS Biomater. Sci. Eng.* **2020**, *6*, 4512.
- [23] Z. N. Mao, X. W. Bi, F. Ye, P. Y. Du, X. Shu, L. Sun, J. Guan, X. M. Li, S. J. Wu, *Int. J. Biol. Macromol.* **2021**, *182*, 1268.
- [24] Z. T. Man, L. Yin, Z. X. Shao, X. Zhang, X. Q. Hu, J. X. Zhu, L. H. Dai, H. J. Huang, L. Yuan, C. Y. Zhou, H. F. Chen, Y. F. Ao, *Biomaterials* **2014**, *35*, 5250.
- [25] H. J. Huang, X. Zhang, X. Q. Hu, Z. X. Shao, J. X. Zhu, L. H. Dai, Z. T. Man, L. Yuan, H. F. Chen, C. Y. Zhou, Y. F. Ao, *Biomaterials* **2014**, *35*, 9608.
- [26] Y. Chen, T. Wu, S. Huang, C. W. Suen, X. Cheng, J. Li, H. Hou, G. She, H. Zhang, H. Wang, X. Zheng, Z. Zha, *ACS Appl. Mater. Interfaces* **2019**, *11*, 14608.
- [27] M. Yamamoto, Y. Ikada, Y. Tabata, *J. Biomater. Sci., Polym. Ed.* **2001**, *12*, 77.
- [28] Z. Luo, L. Jiang, Y. Xu, H. Li, W. Xu, S. Wu, Y. Wang, Z. Tang, Y. Lv, L. Yang, *Biomaterials* **2015**, *52*, 463.
- [29] X. Sun, H. Yin, Y. Wang, J. J. Lu, X. Z. Shen, C. F. Lu, H. Tang, H. Y. Meng, S. H. Yang, W. Yu, Y. Zhu, Q. Y. Guo, A. Y. Wang, W. J. Xu, S. Y. Liu, S. B. Lu, X. M. Wang, J. Peng, *ACS Appl. Mater. Interfaces* **2018**, *10*, 38715.
- [30] Y. T. Wen, N. T. Dai, S. H. Hsu, *Acta Biomater.* **2019**, *88*, 301.
- [31] S. S. Lee, J. H. Kim, J. Jeong, S. H. L. Kim, R. H. Koh, I. Kim, S. Bae, H. Lee, N. S. Hwang, *Biomaterials* **2020**, *257*, 120223.
- [32] X. Liu, Y. Wei, C. Xuan, L. Liu, C. Lai, M. Chai, Z. Zhang, L. Wang, X. Shi, *Adv. Healthcare Mater.* **2020**, *9*, 2000076.
- [33] Z. Shao, X. Zhang, Y. Pi, X. Wang, Z. Jia, J. Zhu, L. Dai, W. Chen, L. Yin, H. Chen, C. Zhou, Y. Ao, *Biomaterials* **2012**, *33*, 3375.
- [34] H. Huang, X. Zhang, X. Hu, Z. Shao, J. Zhu, L. Dai, Z. Man, L. Yuan, H. Chen, C. Zhou, Y. Ao, *Biomaterials* **2014**, *35*, 9608.
- [35] C. Erggelet, M. Endres, K. Neumann, L. Morawietz, J. Ringe, K. Haberstrohm, M. Sittlinger, C. Kaps, *J. Orthop. Res.* **2009**, *27*, 1353.
- [36] C. H. Lee, J. L. Cook, A. Mendelson, E. K. Moiola, H. Yao, J. J. Mao, *Lancet* **2010**, *376*, 440.
- [37] M. Chen, Y. Li, S. Liu, Z. Feng, H. Wang, D. Yang, W. Guo, Z. Yuan, S. Gao, Y. Zhang, K. Zha, B. Huang, F. Wei, X. Sang, Q. Tian, X. Yang, X. Sui, Y. Zhou, Y. Zheng, Q. Guo, *Bioact. Mater.* **2021**, *6*, 1932.
- [38] H. T. Xia, D. D. Zhao, H. L. Zhu, Y. J. Hua, K. Y. Xiao, Y. Xu, Y. Q. Liu, W. M. Chen, Y. Liu, W. J. Zhang, W. Liu, S. J. Tang, Y. L. Cao, X. Y. Wang, H. H. Chen, G. D. Zhou, *ACS Appl. Mater. Interfaces* **2018**, *10*, 31704.
- [39] L. Li, J. Y. Li, J. M. Guo, H. K. Zhang, X. Zhang, C. Y. Yin, L. M. Wang, Y. S. Zhu, Q. Q. Yao, *Adv. Funct. Mater.* **2019**, *29*, 1807356.
- [40] A. C. Bakker, F. A. J. van de Loo, H. M. van Beuningen, P. Sime, P. L. E. M. van Lent, P. M. van der Kraan, C. D. Richards, W. B. van den Berg, *Osteoarthr. Cartilage* **2001**, *9*, 128.
- [41] H. M. van Beuningen, H. L. Glansbeek, P. M. van der Kraan, W. B. van den Berg, *Osteoarthr. Cartilage* **2000**, *8*, 25.
- [42] G. Cheng, J. H. Dai, J. W. Dai, H. Wang, S. Chen, Y. H. Liu, X. Y. Liu, X. R. Li, X. Zhou, H. B. Deng, Z. Li, *Chem. Eng. J.* **2021**, *410*, 128379.
- [43] C. Levinson, M. Lee, L. A. Applegate, M. Zenobi-Wong, *Acta Biomater.* **2019**, *99*, 168.
- [44] C. J. Little, N. K. Bawolin, X. B. Chen, *Tissue Eng.* **2011**, *17*, 213.
- [45] Z. Z. Zhang, Y. R. Chen, S. J. Wang, F. Zhao, X. G. Wang, F. Yang, J. J. Shi, Z. G. Ge, W. Y. Dingo, Y. C. Yang, T. Q. Zou, J. Y. Zhang, J. K. Yu, D. Jiang, *Sci. Transl. Med.* **2019**, *11*, eaao0750.
- [46] M. J. Gu, S. N. Fan, G. D. Zhou, K. Ma, X. Yao, Y. P. Zhang, *Composites, Part B* **2022**, *235*, 1097644.
- [47] X. L. Ouyang, Y. F. Xie, G. H. Wang, *Biomed. Pharmacother.* **2019**, *117*, 109146.
- [48] Q. T. Li, S. Xu, Q. Feng, Q. Y. Dai, L. T. Yao, Y. C. Zhang, H. C. Gao, H. Dong, D. F. Chen, X. D. Cao, *Bioact. Mater.* **2021**, *6*, 3396.